


# Room-temperature multiferroic behavior in layer-structured Aurivillius phase ceramics

Cite as: Appl. Phys. Lett. **117**, 052903 (2020); <https://doi.org/10.1063/5.0017781>

Submitted: 09 June 2020 . Accepted: 25 July 2020 . Published Online: 07 August 2020

Zheng Li, Vladimir Koval , Amit Mahajan, Zhipeng Gao, Carlo Vecchini, Mark Stewart, Markys G. Cain , Kun Tao, Chenglong Jia , Giuseppe Viola, and Haixue Yan 



View Online



Export Citation



CrossMark

## ARTICLES YOU MAY BE INTERESTED IN

[Intrinsic piezoelectricity in \(K,Na\)NbO<sub>3</sub>-based lead-free single crystal: Piezoelectric anisotropy and its evolution with temperature](#)

Applied Physics Letters **117**, 052904 (2020); <https://doi.org/10.1063/5.0012124>

[Current-induced bulk magnetization of a chiral crystal CrNb<sub>3</sub>S<sub>6</sub>](#)

Applied Physics Letters **117**, 052408 (2020); <https://doi.org/10.1063/5.0017882>

[Magnetic transition behavior and large topological Hall effect in hexagonal Mn<sub>2-x</sub>Fe<sub>1+x</sub>Sn \(x = 0.1\) magnet](#)

Applied Physics Letters **117**, 052407 (2020); <https://doi.org/10.1063/5.0011570>



**Measure Ready**  
**FastHall™ Station**

The highest performance tablet system...  
for van der Pauw and Hall bar samples

[Learn more](#)

Lake Shore  
CRYOTRONICS

AIP

Publishing

# Room-temperature multiferroic behavior in layer-structured Aurivillius phase ceramics

Cite as: Appl. Phys. Lett. **117**, 052903 (2020); doi: [10.1063/5.0017781](https://doi.org/10.1063/5.0017781)

Submitted: 9 June 2020 · Accepted: 25 July 2020 ·

Published Online: 7 August 2020 · Corrected: 11 August 2020



View Online



Export Citation



CrossMark

Zheng Li,<sup>1</sup> Vladimir Koval,<sup>2</sup> Amit Mahajan,<sup>3</sup> Zhipeng Gao,<sup>4</sup> Carlo Vecchini,<sup>5</sup> Mark Stewart,<sup>5</sup> Markys G. Cain,<sup>6</sup> Kun Tao,<sup>7</sup> Chenglong Jia,<sup>7,a)</sup> Giuseppe Viola,<sup>3</sup> and Haixue Yan<sup>3,b)</sup> 

## AFFILIATIONS

<sup>1</sup> Graduate School of Materials Science and Engineering, Beijing University of Aeronautics and Astronautics, Beijing 100074, China

<sup>2</sup> Institute of Materials Science and Engineering, A\*STAR, Singapore 117602, Singapore

<sup>3</sup> Department of Materials Science and Engineering, University of California, Los Angeles, California 90095, USA

<sup>4</sup> National Key Laboratory of Materials Physics, Institute of Physics, Chinese Academy of Sciences, Beijing 100080, China

<sup>5</sup> Department of Materials Science and Engineering, University of California, Los Angeles, California 90095, USA

<sup>6</sup> Department of Materials Science and Engineering, University of California, Los Angeles, California 90095, USA

<sup>7</sup> Department of Materials Science and Engineering, University of California, Los Angeles, California 90095, USA

a) Email: [cljia@ucla.edu](mailto:cljia@ucla.edu)

b) Author to whom correspondence should be addressed: [hyan@ucla.edu](mailto:hyan@ucla.edu)

## ABSTRACT

Multiferroic behavior is observed in layer-structured Aurivillius phase ceramics  $B_{5.25}L_{0.75}F_{1-x}C_xO_{18}$  ( $x = 0, 0.25, 0.5, 0.75, 1$ ) at room temperature. The  $B_{5.25}L_{0.75}F_{1-x}C_xO_{18}$  ceramics exhibit a transition from a paraelectric (PE) state to a ferroelectric (FE) state at room temperature. The transition temperature  $T_c$  increases with the  $C/F$  ratio. The  $B_{5.25}L_{0.75}F_{1-x}C_xO_{18}$  ceramics exhibit a transition from a paraelectric (PE) state to a ferroelectric (FE) state at room temperature. The transition temperature  $T_c$  increases with the  $C/F$  ratio. The  $B_{5.25}L_{0.75}F_{1-x}C_xO_{18}$  ceramics exhibit a transition from a paraelectric (PE) state to a ferroelectric (FE) state at room temperature. The transition temperature  $T_c$  increases with the  $C/F$  ratio.

Published under license by AIP Publishing. <https://doi.org/10.1063/5.0017781>

Multiferroic behavior is observed in layer-structured Aurivillius phase ceramics  $B_{5.25}L_{0.75}F_{1-x}C_xO_{18}$  ( $x = 0, 0.25, 0.5, 0.75, 1$ ) at room temperature. The  $B_{5.25}L_{0.75}F_{1-x}C_xO_{18}$  ceramics exhibit a transition from a paraelectric (PE) state to a ferroelectric (FE) state at room temperature. The transition temperature  $T_c$  increases with the  $C/F$  ratio. The  $B_{5.25}L_{0.75}F_{1-x}C_xO_{18}$  ceramics exhibit a transition from a paraelectric (PE) state to a ferroelectric (FE) state at room temperature. The transition temperature  $T_c$  increases with the  $C/F$  ratio. The  $B_{5.25}L_{0.75}F_{1-x}C_xO_{18}$  ceramics exhibit a transition from a paraelectric (PE) state to a ferroelectric (FE) state at room temperature. The transition temperature  $T_c$  increases with the  $C/F$  ratio.

$B_{5.25}L_{0.75}F_{1.0}C_{1.0}O_{18}$   
 $(BLFC)$   
 $a, b$   
 $a = 5.4530(2) \text{ \AA}, b = 5.4427(1) \text{ \AA}$   
 $c = 50.670(2) \text{ \AA}$   
 $b = 5.3943(6) \text{ \AA}, c = 41.487(2) \text{ \AA}$

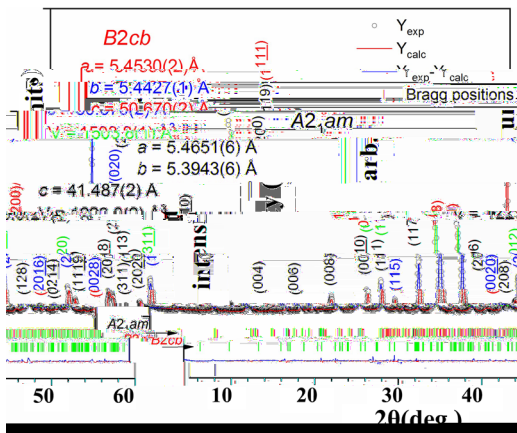


FIG. 1. XRD pattern of BLFC.

$B_{5.25}L_{0.75}F_{1.0}C_{1.0}O_{18}$   
 $(BLFC)$   
 $a, b$   
 $a = 5.4530(2) \text{ \AA}, b = 5.4427(1) \text{ \AA}$   
 $c = 50.670(2) \text{ \AA}$   
 $b = 5.3943(6) \text{ \AA}, c = 41.487(2) \text{ \AA}$

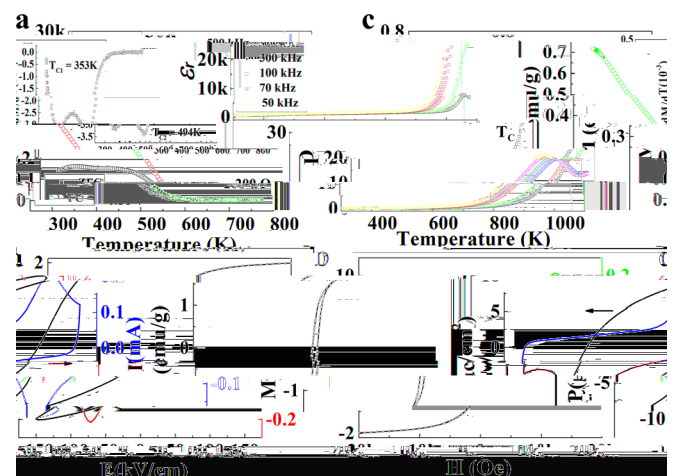


FIG. 2. Temperature dependence of dielectric loss (D), piezoelectric coefficient (P), and pyroelectric coefficient (Pc) for BLFC.

$\sim 494$  K (M/),  
 $B_6F_2C_{18}O_{18}$  (526 K).<sup>23</sup>  
 BLFC  
 $F^{3+} O F^{3+}, C^{3+} O C^{3+}, F^{3+} O C^{3+}$  (.  
 ED).<sup>24</sup>  
 A FC  $\sim 353$  K  
 $C_2F_2O_4$   $\sim 2$  (M)  $C_2F_2O_4$  <sup>16,25</sup>  
 $C_2F_2O_4$  (460 K)  
 $16.235 / .$ <sup>25</sup> ,  $0.22 0.32 / , 1.4 .\%$   
 $C_2F_2O_4$   
 $M = 1.85 / , F . 2( 1. I$   
 $\sim 2 (F . 3) .$   
 $425$  K  $1.58 / .$   
 $0.27 / ,$   
 ED  
 BLFC  
 A  
 $F 3$   
 $(DF)$   $F^{3+} O C^{3+}$  *ab initio*  
 $(A)$   $H$   
 $\mu_F = 2$   $\mu_C = 3$   $F C$  ,  
 $(GGA)+\mu$  . I  
 BLFC  
 $F . 3( 1, F^{3+} C^{3+} (3.1 2.1 \mu_B/ , )$  ,  
 $( 0.1 \mu_B/ ) .$   
 $F O_6 C O_6$   
 $( ) F / C$   
 $F O - / F . 3( 1. I$   
 $F F^{3+} C^{3+}$   
 $( . , )$  ,  
 $( )$  ,  
 $E_{FM} - E_{AFM}$   
 $= -144.1 .$   
 $H$  ,  $(FM)$   
 $43.5 ( . , 504.6 K)$  , FM  
 $\sim 1 FC/FC . F . 2( 1. I$   
 $a b$   
 $010$   
 BLFC  $F 4$  . I  
 $399 O .$   
 $F .$   
 $F -$

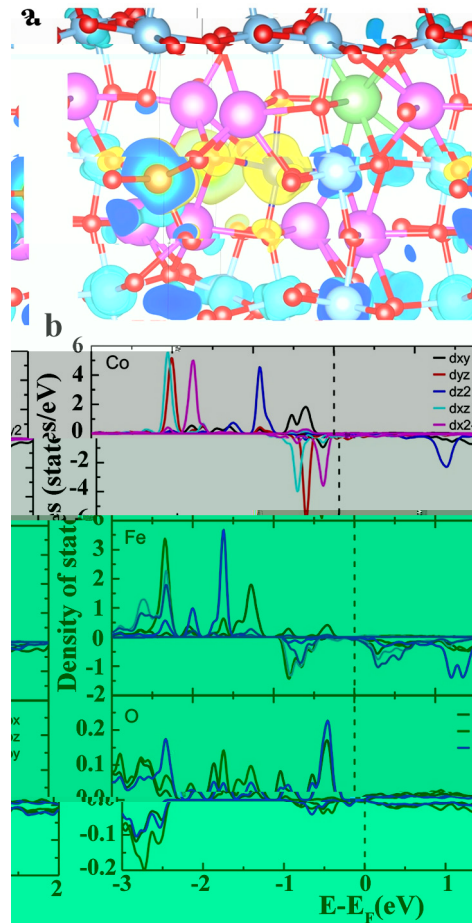


FIG. 3. (a) Crystal structure of BLFC. (b) Density of states (DOS) for Co, Fe, and O atoms. The DOS is calculated using the GGA+U method with  $U = 0.005$  eV. The legend indicates the contributions of different orbitals:  $d_{xy}$  (black),  $d_{yz}$  (red),  $d_{z^2}$  (blue),  $d_{xz}$  (cyan), and  $d_{x^2-y^2}$  (magenta).

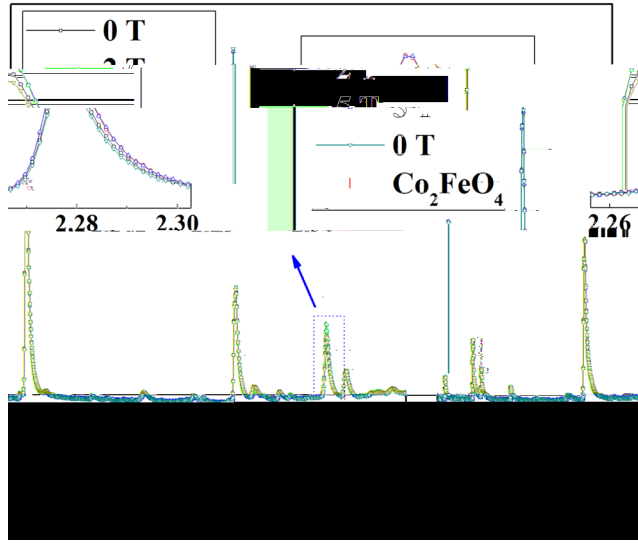


FIG. 4. XRD patterns of  $\text{Co}_2\text{FeO}_4$  at 0 T and 2 T. The inset shows the schematic of the sample and measurement setup.

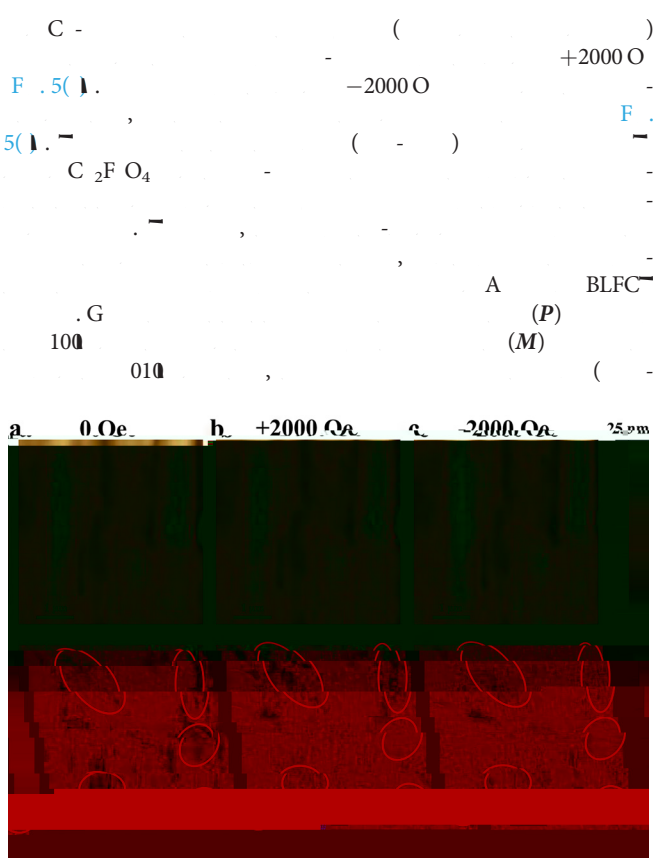


FIG. 5. MFM images of  $\text{Co}_2\text{FeO}_4$  at 0 Oe, +2000 Oe, and -2000 Oe. The scale bar is 25.0 nm.

$T = P \times M$   
 BLFC<sup>-</sup>  
 I , A BLFC<sup>-</sup>  
 F  
 $\text{C}^{3+} \text{O} \text{C}^{3+}, \text{F}^{3+} \text{O} \text{C}^{3+}$   
 $\text{F}^{3+} \text{O} \text{F}^{3+}$   
 A , C / F  
 EM (ED )  
 BLFC<sup>-</sup>  
 D . M , D . K , D .  
 D I H I I N , AL,  
 D , O , K .  
 A E D F  
 G A A (G N . 2/  
 0038/20), C (G N . K2015-0602006), N FC (G  
 N . 11474138 11834005). A  
 E M (EM )  
 IND54 N EM  
 EM E AME E

DATA AVAILABILITY

REFERENCES

1. E , N. D. M , J. F. , N 442, 759 (2006).
2. N. A. , N . M . 6, 21 (2007).
3. M , J. H , . L , C . N , A . M . 23, 1062 (2011).
4. L. F. H , O. C , J. B , J. L , , C. H , .  
H , H , O. G , D. C. L , H. , K ,  
A. J. B , A . F . M . 26, 2111 (2016).
5. N. A. H , J. . C . B 104, 6694 (2000).
6. B. A , M : II.  
B<sub>4</sub>-<sub>3</sub>O<sub>12</sub>, A . K 1(58), 499 512 (1949).
7. A , G. K , M. M. K , J. . : C  
M . 11, 3335 (1999).
8. N . G. . K , M . . E . B 108, 194 (2004).
9. L. K , M , M. , A. A , N. D , N. , M.  
E. , D. J , J. A . C . . 96, 2339  
(2013).
10. L. J. M , . G , G. , K , A. M , . L , C. J , C. N ,  
H. , D . 45, 14049 (2016).
11. J. F. , N GA M . 5, 72 (2013).
12. A. B C. E , B 90, 214109 (2014).
13. J. B. L. , . H , G. H. , G. . L , J. L , J. C , J. K. L ,  
A . . L . 96, 222903 (2010).
14. M , . C , . L , A . . L . 95, 082901 (2009).
15. L. J. , . L , . J. D , . , A . . L .  
101, 122402 (2012).

- <sup>16</sup>M. , C. , M. B. , A. B. , J. H. , K. , L. K. , M. , C. , H. K. , A. J. B. , *J. A. C.* **112**, 073919 (2012).
- <sup>17</sup>J. L. , H. , M. J. , K. , *J. A. C.* **102**, 104107 (2007).
- <sup>18</sup>M. G. C. , *Characterisation of Ferroelectric Bulk Materials and Thin Films* ( , 2014), .2.
- <sup>19</sup>.L., K. , J. M. , G. , K. , C. J. , G. , H. , A. M. , J. C. , M. C. , I. A. , C. N. , C. J. , H. , *J. M. C. C.* **6**, 2733 (2018).
- <sup>20</sup>.K. , I. , G. , M. , C. J. , H. , *J. A. C.* **122**, 15733 (2018).
- <sup>21</sup>L. J. , F. L. , *J. A. C.* **97**, 1 (2014).
- <sup>22</sup>H. , F. I. , G. , H. N. , H. , J. , G. , M. J. , *J. A. D.* **1**, 107 (2011).
- <sup>23</sup>J. , L. , L. , J. D. , A. , *L.* **101**, 012402 (2012).
- <sup>24</sup>B. , J. , J. C. , L. , J. D. , A. , *L.* **104**, 062413 (2014).
- <sup>25</sup>L. M. , N. B. , *L.* **11**, 719 (2009).